Research article

Interaction between methyl red and cetyltrimethylammonium bromide under the influence of sodium polystyrene sulphonate in ethanol-water binary solvent systems: A spectrophotometric investigation

Shiv Narayan Yadav [a,b], Summi Rai [a,c], Ajaya Bhattarai [a,*], Biswajit Sinha [b,**]

[a] Department of Chemistry, Mahendra Morang Adarsh Multiple Campus, Tribhuvan University, Biratnagar, 56613, Nepal
[b] Department of Chemistry, University of North Bengal, Darjeeling, 734013, India
[c] National Archives, Ministry of Culture, Tourism and Civil Aviation, Government of Nepal, Kathmandu, 44600, Nepal

ARTICLE INFO

ABSTRACT

This research aims to comprehensively investigate and analyze the UV–visible spectroscopic behavior of the methyl red (MR)-cetyltrimethylammonium bromide (CTAB) system under the influence of sodium polystyrene sulfonate (NaPSS) in aqueous and different volume fractions (v. f.) of ethanol (EtOH)–H_2O (0.1, 0.2, and 0.3) at 298.15 ± 0.2 K. In EtOH–H_2O solvent systems, the triple interactions of dyes-surfactants-polyelectrolyte (DSP) complex systems are entirely novel. MR interacts with CTAB in NaPSS in the binary solvent media (0.1, 0.2, and 0.3 v.f. of EtOH–H_2O) resulting in the formation of ion-pairs at very low CTAB concentrations, far below their apparent critical micelle concentration (CMC*) reducing the absorbance, and the new complexes above the CMC* due to solubilization of the MR into CTAB micelles observed by distinct spectral shifts. The CMC* values obtained from spectroscopic data increase in the order: $(CMC^*)_{water} < (CMC^*)_{0.1} < (CMC^*)_{0.2} < (CMC^*)_{0.3}$. This is because of the reduced polarity or dielectric constant and increased degree of water structure disruption around the hydrophobic chains of CTAB, where micelle formation occurs at somewhat higher concentrations. The Gibbs energy of micellization (ΔG_m^o) increases in the order: $(\Delta G_m^o = -16.89)_{water} < (\Delta G_m^o = -16.17)_{0.1} < (\Delta G_m^o = -15.62)_{0.2} < (\Delta G_m^o = -15.38)_{0.3}$, which further supports the inhibitory effect of increasing ethanol content towards micellization. In the post-micellar region, the decrease in hydrophobic interactions and an increase in electrostatic interactions lead to a rise in the overall binding constant value. This means that, when NaPSS is present, the stronger electrostatic interactions in the post-micellar region contribute significantly to the increased binding of CTAB micelles with MR. The tautomeric activity of MR and the solvent composition played a prime role in affecting the interaction mechanism, as evidenced by the blue and red spectral shifts.

* Corresponding author.
** Corresponding author.
E-mail addresses: ajaya.bhattarai@mmamc.tu.edu.np (A. Bhattarai), biswachem@gmail.com (B. Sinha).

1. Introduction

The study of molecular interactions between organic dyes and surfactants with polyelectrolytes gathers considerable attention due to their significant implications in various fields, including pharmaceuticals, materials science, environmental remediation, and industrial processes. Surfactant-polymer, polymer-dye, and dye-surfactant are highly prevalent in surface chemistry research because so many investigations are documented utilizing water as a medium [1–7]. The present investigation deals with the triple interactions of the dye-surfactant-polyelectrolyte (DSP) complex system in ethanol-water (EtOH–H₂O) solvent media.

Methyl red (MR), a pH and solvent-polarity-sensitive azo dye (–N=N–) sometimes referred to as C.I. red 2, is widely investigated for its spectroscopic behavior and interactions with various chemical species [8,9]. The basic form of MR is an anionic (deprotonated acid) known as MR⁻, while its acid form is zwitterionic (protonated form) known as HMR, as shown in Fig. 1 [10,11]. MR is a good fit for our system since both its acidic and basic forms show prominent peaks in the UV–visible spectrum [12]. In an acidic environment, the lone pair of electrons on the nitrogen of the dimethylamino group accepts a proton, forming $–NH(CH_3)_2^+$. This protonation increases the electron density on the azo group and the aromatic ring to which it is attached, altering the electron distribution. The altered electron distribution shifts the absorption spectrum of the molecule, causing it to absorb light in a way that appears red color. In a basic environment, the carboxylic acid group loses a proton, forming -COO⁻. This deprotonation reduces the electron density on the azo group and the aromatic ring, changing the electronic structure. The new electron distribution shifts the absorption spectrum of the molecule, resulting in the molecule absorbing light in a way that appears yellow [9,10,13].

Cetyltrimethylammonium bromide (CTAB), is a cationic surfactant known for its versatile applications, particularly in micellar systems and colloidal science [14,15]. The numerical value of the CMC of the surfactant plays a critical role in describing the adsorption and solubilization behavior of the micellar solutions [16]. In this context, sodium polystyrene sulphonate (NaPSS), a water-soluble strong anionic polyelectrolyte known for its hydrophobic character (due to PSS⁻) with external hydrophobic domains and diverse applications, emerges as a noteworthy additive [17–19]. Surfactant interacts with polyelectrolytes, macromolecules, and dye, a colorant (having chromophores and auxochromes) [20,21]. The addition of NaPSS to the MR-CTAB system is anticipated to introduce variations in the molecular interactions, potentially affecting the nature and stability of the formed complexes. A substantial amount of CTA⁺ is absorbed on the NaPSS surface upon the progressive addition of CTAB, raising the positive (+ve) charge on the substance. This leads to the formation of the (CTA⁺PSS⁻) complex and the release of counterions from the CTAB micelle and polyelectrolyte ions [17,18].

Understanding these alterations may offer novel perspectives on the behavior of such complex systems and their applicability in tailored environments. Electrostatic interactions, hydrogen bonding, hydrophobic interactions, and van der Waals forces are the intermolecular forces that control the solubilization process of the dyes [16,22]. Hydrophobic interactions, and electrostatic interactions [23,24], play a vital role in the system's behavior and performance [25–28].

These interactions are influenced by the nature of the dye and surfactant and the medium in which they are dissolved. Solvent systems and additives are crucial to the molecular assembly, aggregation, and stability of the dye-surfactant complexes. Water and EtOH–H₂O binary solvent systems are widely recognized for their varying polarity and interaction capabilities. The unique solvent properties via hydrogen bonding can significantly impact the nature and extent of interactions between molecules dissolved within
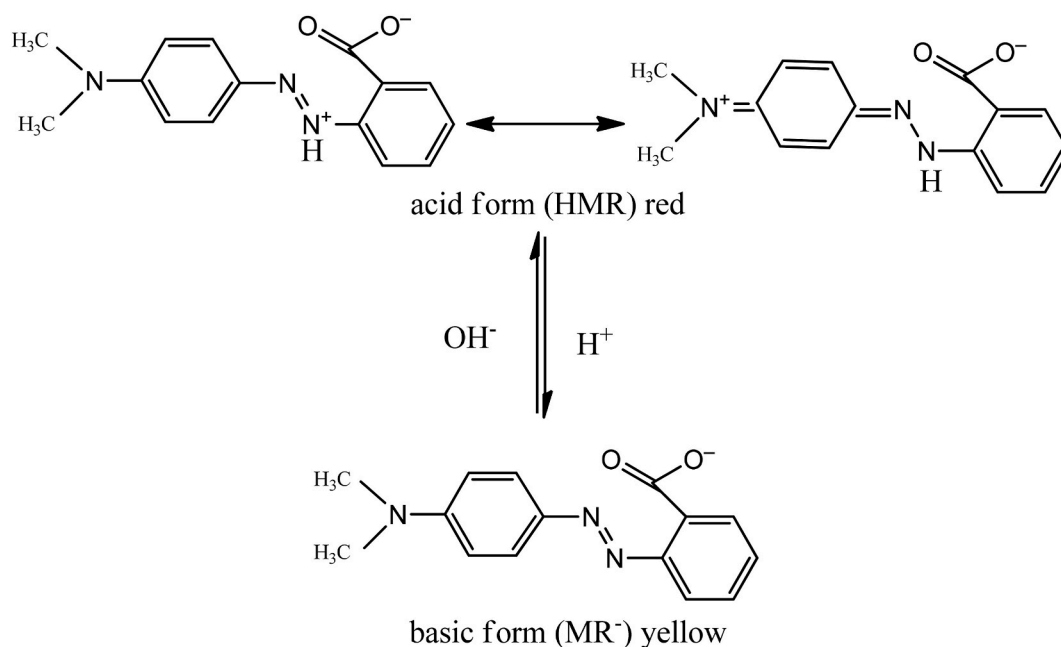

Fig. 1. Acid and basic forms of Methyl red.

them [29]. Exploring the interaction between methyl red and CTAB/NaPSS in these solvent systems provides an opportunity to elucidate the influence of solvent polarity and composition on their association behavior. As ethanol reduces hydrophobic affinity, it causes changes in cohesion energy, water structure, dye solvation preference, micelle size, and chemical stability, which consequently affects binding constant, spectral shift, CMC, etc. [30–33]. Consequently, ethanol has been chosen as the solvent of interest to study these effects because it is a crucial chemical and pharmaceutical solvent.

We use a UV–visible spectroscopy approach to accomplish our objective owing to its exceptional sensitivity, precision, and accuracy, toward molecular affinity and properties [27,34–36]. The dye addition may influence the surfactants' micellization properties, resulting in the determination of an apparent CMC (CMC*) rather than actual CMC [36].

Previous studies [10,18,37–42] suggested the possibility of complex formation between methyl red and CTAB, leading to spectral changes that reflect alterations in the dye's electronic environment. However, a comprehensive investigation into the spectroscopic characteristics and the nature of the interaction between these species under the influence of NaPSS in different solvent environments remains a significant gap in the current understanding. We are thus inspired to study the interaction of MR with CTAB under the influence of NaPSS by spectroscopic studies in water and in different volume fractions of EtOH–H$_2$O (0.1, 0.2, and 0.3) at 298.15 ± 0.2 K. The spectral changes, binding constant (K_b), CMC*, Gibbs energy of binding (ΔG_b^o), and Gibbs energy of micellization (ΔG_m^o) obtained from these studies are expected to provide crucial insights into the molecular level interactions occurring within these systems. The results of this study greatly advance our understanding of the complex interactions between molecules, and their implications in diverse scientific, industrial, ecological, pharmaceutical, and technological domains. It will also pave the way for future studies on the effects of various co-solvents and other additives in the dye-surfactant-polyelectrolyte (DSP) interaction for the production of new, advanced, and sustainable materials with enhanced yield and economy for relevance to society.

2. Experimental

2.1. Materials

Table 1 displays the names, companies, and countries of the purchased chemicals, along with the CAS number, molecular weight, and purity percentage.

2.2. Methods

The EtOH–H$_2$O mixed solvent media (0.1, 0.2, and 0.3) were prepared using triple distilled water. CTAB (0.004 mol L^{-1}), NaPSS (0.0001 mol L^{-1}), and MR (5×10^{-5} mol L^{-1}) stock solutions were made in water, and 0.1, 0.2, and 0.3 fractions of the EtOH–H$_2$O volume, respectively. The corresponding solvent media were used to prepare CTAB in NaPSS at various concentrations (0.00055–0.003667 mol L^{-1}). 2 mL of MR solution was added to different concentrations of CTAB solutions [41,43]. As a result of this preparation, the final concentration of MR is 4.16×10^{-6} mol L^{-1}. A double-beam (MARS, ME-SP, 195UV, India) UV–visible spectrophotometer fitted with a quartz cuvette with a length of 10 mm was used to obtain the absorption spectra. MR spectra were recorded at 298.15 ± 0.2 K between 200 and 800 nm, while the spectra were taken between 350 and 600 nm for clear visibility. The maximum absorbance of MR in water was found in the range of 432–438 nm, which is consistent with the literature [10,44].

3. Results and discussion

3.1. Absorption spectra of MR in different solvent media

The nature and polarity of the binding sites can be inferred from the spectral features of the MR-CTAB-NaPSS solution [22]. The hydrophobic property of the aromatic ring of MR is important in probing the relationship between physicochemical properties and molecular architecture [12].

3.1.1. In water

Dyes show notable spectrum shifts in different micellar regions of the surfactant/polyelectrolyte system [45,46]. Two regions are taken regarding the spectral shift of the MR with increasing CTAB concentration: First, CTAB concentration is far below CMC* because

Table 1
Details of the chemicals used.

Names of chemicals	Sources of chemicals	CAS number of chemicals	Mol. Wt. (g mol^{-1})	Purity percentage
Sodium polystyrene sulfonate [NaPSS]	Sigma Aldrich, USA	25704-18-1	70,000.00	99.5 %
Cetyltrimethlammoniumbromide [CTAB]	Sigma Aldrich, USA	57-09-0	364.45	$\geq$ 98.0 %
Methyl Red [MR]	B.D.H. Laboratory Chemicals, Poole, England	981010	269.30	99.5 %
Ethanol	E. Merck, India	64-17-5	46.48	$\geq$ 99.0 %

cluster or ion-pairs (CTAB$^+$MR$^-$) or the dimer of MR are formed in this region [39,47], reducing the absorbance at $\lambda_{\max}$, and second, CTAB concentration is above CMC* because the dye solubilizes into micelle.

The dye (MR) shows a 432–438 nm maximum absorbance ($\lambda_{\max}$) in the aqueous solution (water) at 298.15 ± 0.2K. This absorption band is caused by the anionic (basic) form of the dye. A single signal in the 432–438 nm region suggests the existence of a monomer form of the dye [12,22] under investigation. The spectral changes are shown in Fig. 2. As the concentration of CTAB increases, the value of $\lambda_{\max}$ of MR decreases with the appearance of new bands within the range of 412–424 nm. This shift in the value $\lambda_{\max}$ with CTAB concentration is a clear signal of the affinity of anionic MR and cationic CTAB, and the formation of the complex between them. This is due to the hypsochromic absorption shift caused by the dye H-aggregates (Fig. 2) [48,49]. Strong π-π intermolecular interactions around the molecules cause them to adopt a nearly parallel shape, which leads to face-to-face stacking and the emergence of the H-aggregate [28,41,50]. Here, the dye's COO$^-$ group and the surfactant's ($> N^+$) are electrostatically interacting, which causes the blue shift [28]. The shift in $\lambda_{\max}$ to 412–424 nm from 0.001724 to 0.000458 mol L^{-1} of CTAB concentration (Fig. 2), shows that CTAB aggregates with MR and releases PSS$^-$ ions, which facilitates micellization [51]. The MR and CTAB seem to produce a strong complex, which shifts the equilibrium between the CTAB and NaPSS complexes [41,52]. In this case, the attractive force between CTA$^+$ and MR$^-$ is stronger than the electrostatic force between CTA$^+$ and PSS$^-$, leading to the disintegration of methyl red dimers and the formation of CTAPSS complex (CTAB + NaPSS) [53]. Here, the less rigid structure of MR helps it fit into the micelle easily. Because of this, micellization is facilitated and the repulsion between the micelle's ionic heads is reduced [28,51]. There is a gradual decrease in absorbance of the dye with CTAB concentration, and a minimum is seen at 0.0011 mol L^{-1} of the CTAB concentration, which is the CMC*. Similar trends of results were also observed in the literature [22,41,43].

The CTA$^+$MR$^-$ complex is formed by the combined effect of electrostatically and hydrophobically interacting forces, which causes a rise in $\lambda_{\max}$ and a decrease in absorbance values [54]. Due to the rapid MR-CTAB ion pair formation, the electrostatically interacting forces between the methyl red molecules become less. This promotes dimerization through hydrophobic forces and London dispersion, lowering absorbance [51,55]. Upon a rise in CTAB concentration, micellization occurs, and the micelles break the methyl red dimers, and MR-CTAB ion pairs are incorporated with the micelles. On further addition of CTAB, MR monomers get associated with these micelles resulting in a rapid rise in absorbance after the CMC*. After additional dye molecules are added to the micelles, the absorbance value approaches a limiting value, reaching near-constant levels [39,56] at 0.000458 mol L^{-1} CTAB concentration, and the solubilization is almost complete, resulting in no further spectral change. Such trends of spectral shifts were also observed in the case of the other dyes/surfactants [39,43,50,55].

In the CTAB-NaPSS system, increasing methanol and NaPSS concentrations causes increases in α, CAC, and CMC*. Furthermore, in the CTAB-NaPSS system, the value of β drops when methanol and NaPSS are added. A decrease in ΔG_t^0 is observed with the addition of methanol, however, -ve increase of ΔG_t^0 is observed with the addition of NaPSS. When methanol is added, ΔG_{ps}^0 increases negatively, but when NaPSS is added, ΔG_{ps}^0 decreases negatively [17]. Furthermore, even though we have maintained the dye concentration, the literature [57] reports that the CMC of the CTAB decreases as the amount of dye in the aqueous CTAB solution increases. It is suggested that aggregation is more advantageous with higher dye levels because all of the ΔG_m^0 values are -ve and climb as the dye concentration increases. Since it is the main cause of the -ve values of the free energy change (ΔG_m^0), the +ve entropy change (ΔS_m^0) that arises during aggregation is the main driver of aggregation. Furthermore, as dye concentration increases at a particular temperature, there may be a +ve change in entropy due to the release of hydrated water molecules surrounding the surfactant monomers.

3.1.2. 2. In different volume fractions (0.1, 0.2, and 0.3) of EtOH–H$_2$O solvent systems

MR shows a remarkable spectral shift in different micellar regions with varying solvent compositions of EtOH–H$_2$O systems. The observed spectra of MR are analyzed below and above the CMC* of CTAB in the dye-surfactant-polyelectrolyte system. The maximum absorbance of MR is observed in the range of 430–440 nm, which suggests the existence of monomeric dye species and is caused by the
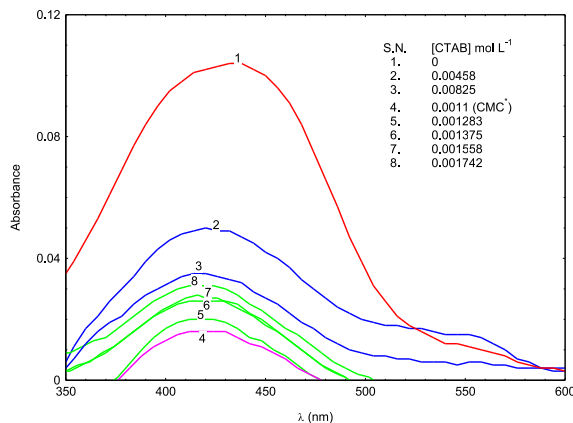

Fig. 2. Absorption Spectra of MR with various CTAB concentrations in water at 298.15 ± 0.2 K.

basic (anionic) form of MR within the concentration range under investigation [58]. Methyl red with CTAB in NaPSS shows a decrease in maximum absorbance with the appearance of the new bands within the range of 405–420 nm, which is a clear indication of the interaction between MR^- and cationic CTA^+, and the formation of the complex between them.

The dielectric constant value becomes smaller with the addition of ethanol in the water. The unique/distinct shift in the intensity or position of a UV/Visible absorption band due to the variation/change in the medium's polarity is known as solvatochromism. When the solvent polarity is increased then λ_{max} shifts towards a shorter wavelength, which shows that the ground state's solvation-free energy is lower than the excited state. This shift is known as the blue or hypsochromic shift. +ve solvatochromism is the result of a redshift occurring with increasing solvent polarity, while -ve solvatochromism is the result of a blue shift occurring with increasing solvent polarity [59].

Therefore, the spectral shift (Fig. 3), which occurs towards a shorter wavelength is called the hypsochromic absorption shift and is due to the -ve solvatochromism [59]. Here, the dye's COO^- group and the surfactant's $(>N^+)$ are electrostatically interacting, which causes the blue shift [28,60]. The shifts in λ_{max} to 405–420 nm from 0.00275 to 0.000917 mol L^{-1} (Fig. 3) of CTAB concentration show that CTAB aggregates with MR and releases PSS^- ions, in 0.1 v.f. of EtOH–H_2O [41,52]. Here micellization becomes slightly difficult in comparison to water due to the decrease in hydrophobic interactions as a result of the reduced dielectric constant of the medium. The absorbance value of the dye gradually decreases with increasing CTAB concentration, and a minimum is seen at 0.0015 mol L^{-1} CTAB concentration, and is the CMC* of the surfactant.

In the 0.2 v.f. of the EtOH–H_2O solvent system, MR shows remarkable spectral changes. The maximum absorbance of MR is observed at 430 nm, which suggests the existence of monomeric dye species and is caused by the anionic version of MR [58]. MR with CTAB in NaPSS shows an increase in maximum absorbance with the appearance of the new bands within the range of 515–525 nm. Therefore, this spectral shift (in the 0.2 v.f. of ethanol-water), which occurs towards a longer wavelength with increasing solvent polarity is due to the bathochromic shift or red shift (+ve solvatochromism) caused by the dye J-aggregates (Fig. 4) [28,48,49,61]. It occurs due to the hydrazone form of MR. The medium's increased polarity signaled the transition from azo to hydrazone form, which also caused the increase in the value of absorbance to some extent [62]. The redshift is a result of the interaction of the MR and the formation of J-aggregates [63–65]. Because of the hydrogen bonding with the azo moiety, the OH^- substituent enhances tautomerism and causes the azo form to shift to the hydrazo form, making the redshift more noticeable. The spectral intersection at a point in Fig. 4 indicates the existence of many isosbestic points for the MR-CTAB-NaPSS system which is proof of MR and CTAB binding [66,67]. An "isosbestic point" is a location in the absorption spectrum that appears during a chemical reaction when the molar absorption coefficients of at least two chemical species are the same. These coefficients remain constant throughout the reaction and in equilibrium, and the concentration of another component controls their relative proportions [66,67]. Some spectra (8&9) showing hypsochromic shift intersect at a point, justifying the isosbestic point as shown in Fig. 4. The value of λ_{max} shifts to 515–525 nm from 0.003117 to 0.0015 mol L^{-1} shows that CTAB aggregates with MR and releases PSS^- ions in 0.2 v.f. of ethanol-water, at lower CTAB concentrations [41,52]. Here micellization becomes more difficult in comparison to water due to the decrease in hydrophobic interactions as a result of the reduced dielectric constant of the medium. The hydrophobic force between CTA^+ and PSS^- becomes much weaker in this case than the electrostatic force between MR^- and CTA^+, which causes the breakdown of methyl red dimers and the CTAPSS complex (CTAB + NaPSS) [53]. The absorbance value of the MR gradually decreases with increasing CTAB concentration, and a minimum is seen at 0.0018 mol L^{-1} CTAB concentration, which is the CMC* in this case. Here, in this case, the CMC* value becomes higher than 0.1 v.f. of ethanol-water.

In the 0.3 v.f. of the EtOH–H_2O solvent system, MR shows a remarkable and interesting spectral shift. The maximum absorbance of methyl red in a 0.3 v.f. of EtOH–H_2O solvent system is observed at 525 nm, which suggests the existence of monomeric dye species and is caused by the acid form (protonated form) of MR [10,58] within the concentration range that is being studied. It occurs due to the hydrazone form of MR. The medium's increased polarity signaled the transition from azo to hydrazone form [62]. MR with CTAB in NaPSS in 0.3 v.f. of EtOH–H_2O shows a slight decrease in maximum absorbance with the appearance of the new bands within the range
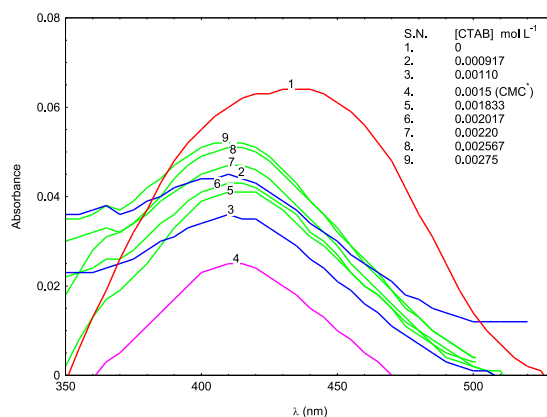

Fig. 3. Absorption Spectra of MR with various CTAB concentrations in 0.1 v.f. of EtOH–H_2O at 298.15 ± 0.2 K.
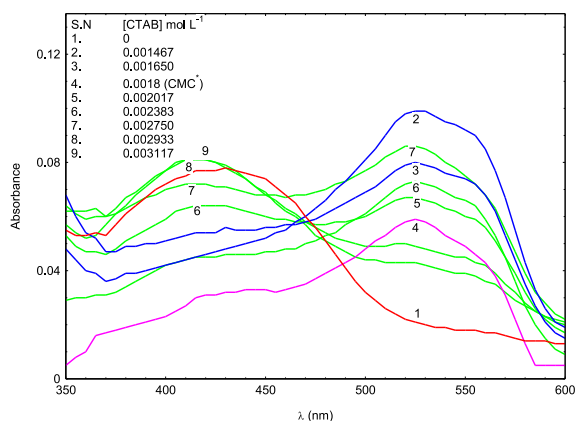
Fig. 4. Absorption spectra of MR with various CTAB concentrations in 0.2 v.f. of EtOH–H$_2$O at 298.15 ± 0.2 K.

of 520–525 nm. Therefore, this spectral shift (in the 0.3 v.f. of ethanol-water), which occurs towards a shorter wavelength with increasing solvent polarity is due to the hypsochromic shift or blue shift (-ve solvatochromism) caused by the dye H-aggregates (Fig. 5). So there occurs a slight blue shift from 525 to 520 nm in the 0.3 v.f. of the EtOH–H$_2$O solvent system, which indicates the interaction between MR$^-$ and cationic CTA$^+$, and the formation of the complex between them. The hypsochromic shift is due to electrostatically interacting forces between the COO$^-$ group of the MR and ($> N^+$) of the CTAB. The shift in λ_{max} shifts to 520–525 nm from 0.003483 to 0.00110 mol L^{-1} (Fig. 5) shows that CTAB aggregates with MR and releases PSS$^-$ ions at lower CTAB concentrations [41,52]. Here micellization becomes more and more difficult in the case of 0.3 v.f. in comparison to water, 0.1, and 0.2 v.f. of ethanol due to the decrease in hydrophobic interactions as a result of the reduced dielectric constant of the medium. The hydrophobic force between CTA$^+$ and PSS$^-$ becomes weaker and weaker in this case than the electrostatic force between MR$^-$ and CTA$^+$, which causes the breakdown of MR dimers and the CTAPSS complex (CTAB + NaPSS). The absorbance value of the dye gradually decreases with increasing CTAB concentration, and a minimum is seen at 0.0020 mol L^{-1}, which is the CMC* with MR.

After micellization, a certain portion of the dye (MR) molecule attaches itself to the micelles in an EtOH–H$_2$O medium, and the dye may experience distinct environmental conditions at the surface or within the micelles compared to an aqueous medium, due to the change in the polarity of the solvent. The absorption spectrum typically shifts when a dye is added to micelles, reflecting the change in the surrounding environment [12,68,69]. Ethanol reduces the micelle formation capacity of CTAB by decreasing the dielectric constant of the medium, which in turn, negatively impacts hydrophobic interaction because it breaks down structured water molecules surrounding the hydrophobic regions of CTAB and MR molecules [27,70]. In addition, ethanol's inhibitory effect is caused by a variety of other mechanisms [71–73].

The electrostatic force between CTA$^+$ and PSS$^-$ becomes stronger with increasing volume fractions of ethanol than hydrophobic interactions, which attract CTA$^+$ and MR$^-$ strongly, which breaks down the dimers of the MR and the CTAPSS complex is formed (CTAB + NaPSS) [53,54]. When the concentration of CTAB is increased, micellization occurs, and the micelles dissociate the MR dimers, and MR-CTAB ion pairs are incorporated with these micelles resulting in the rapid rise in absorbance after the CMC*. The further incorporation of the MR into the micelles causes no spectral change in the absorbance and stays almost constant [39,56], which indicates the completion of the solubilization at the concentrations of CTAB 0.000458, 0.000917, 0.001467, and 0.001100 mol L^{-1}
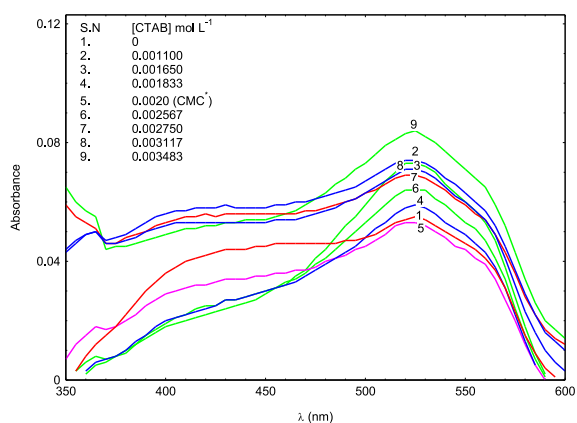

Fig. 5. Absorption spectra of MR with various CTAB concentrations in 0.3 v.f. of EtOH–H$_2$O at 298.15 ± 0.2 K.

respectively for increasing ethanol content (water, 0.1, 0.2, and 0.3) in the solvent. Such trends of spectral shifts were also observed in the case of the other dye/surfactants [39,43,50,55].

3.1.3. Determination of critical micelle concentration (CMC*)

The CMC* displays the concentration at which amphiphilic molecules (surfactant) coalesce into larger spherical aggregates called micelles [74–76]. More stability is associated with a lower CMC* [77].

The higher the solubilization characteristics of hydrophobic species in the solutions, the lower the CMC* value [78]. Because it is used to assess and compare the effectiveness of surface active agents for their intended uses, the CMC* for a surfactant in a particular solvent is, therefore, a prime technique of surfactant characterization [27,35]. Different techniques like conductivity [22], surface tension [19], density, viscosity [30], UV–vis [22,28,35,39,51,55], NMR [79], absorbance, and fluorescence [47,80] have been used for determining the CMC of surfactants.

Two regions are taken regarding the spectral shift of the MR with increasing CTAB concentration: First, CTAB concentration far below CMC* because cluster or ion-pair (CTA^+MR^-) or the dimer of methyl red is formed in this region [39,47], reducing the absorbance at λ_{max}, and second, CTAB concentration above CMC* because the dye solubilizes into micelle.

The addition of methyl red in CTAB solution under the influence of NaPSS results in the creation of clusters of MR or the dimer of MR or MR-CTAB ion-pair due to the combined hydrophobically and electrostatically interacting forces. As a result, a shift in λ_{max} and reduction in absorbance occurs initially far below CMC* of CTAB [25,47,54]. On further addition of CTAB, micellization occurs, and the minimal absorbance value is taken as CMC* (Figs. 6–9), which are tabulated in the table (Table 2). At this point, the micelles dissociate the dimers, and MR-CTAB ion pairs are incorporated with the micelles. On further addition of CTAB, MR monomers get associated with these micelles resulting in the rapid rise in absorbance after the CMC* [51,55]. The further incorporation of the MR into the micelles at higher CTAB concentrations causes no spectral change in the absorbance and stays almost constant [39,56], which indicates the completion of the solubilization at the concentrations of CTAB (0.000458, 0.000917, 0.001467, and 0.001100 mol L^{-1} respectively for increasing ethanol content (water, 0.1, 0.2, and 0.3) in the solvent. Such trends of spectral shifts were also observed in the case of the other dye/surfactants [39,43,50,55].

3.2. Effect of ethanol on CMC*

From the plot of absorbance versus CTAB concentration (Figs. 6–9), the minimal value of the absorbance is taken as CMC* [22,28, 39]', and the CMC* value for the different solvent systems under investigation increases with increasing ethanol content (Table 2). The dielectric constant, or polarity, decreases as the amount of EtOH in the medium increases [81]. The least polarity is in the 0.3 v.f. of ethanol. So CMC* obtained from spectroscopic data follows the order (Table 2): (CMC*)$_{water}$ < (CMC*)$_{0.1}$ < (CMC*)$_{0.2}$ < (CMC*)$_{0.3}$. This is because hydrophobic surfactant chains experience a greater extent of water structure breakage than hydrophilic moieties do, resulting in the formation of micelles at slightly higher concentrations. Similar trends of results are also observed in the literature [18, 19]. The values of CMC* are obtained from spectroscopic data when plotted against different volume fractions of EtOH–H_2O (Fig. 10) then it gives the best fitting of the curve with correlation coefficient, with $r^2 = 1$.

The polarity of the medium drops with increasing ethanol content, and the micelles expand, which causes the increase in electrostatically interacting forces between the ionic head groups in the micelle, and the gradual decrease in hydrophobically interacting forces between the hydrophobic groups of surfactants [82], i.e. the micellization tendency reduces [83].

The Gibbs energy is also determined by taking the CMC* values, using the equation [17]:

$$\Delta G_m^o = RT \ln CMC^* \tag{1}$$

which follows the order: $(\Delta G_m^o)_{water} < (\Delta G_m^o)_{0.1} < (\Delta G_m^o)_{0.2} < (\Delta G_m^o)_{0.3}$ (Table 2). Similar trends are also observed in the literature

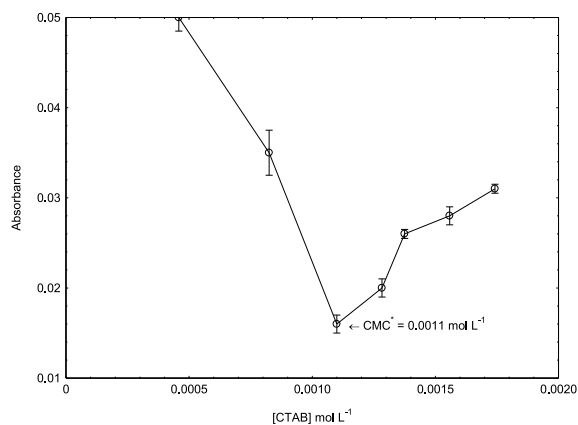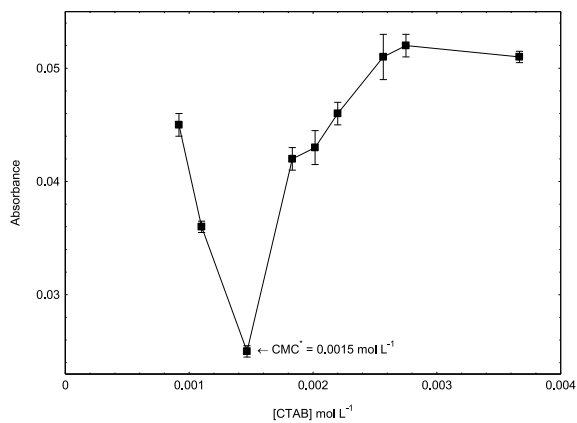**Fig. 6.** The change in absorbance with various CTAB concentrations in water at 298.15 ± 0.2 K.

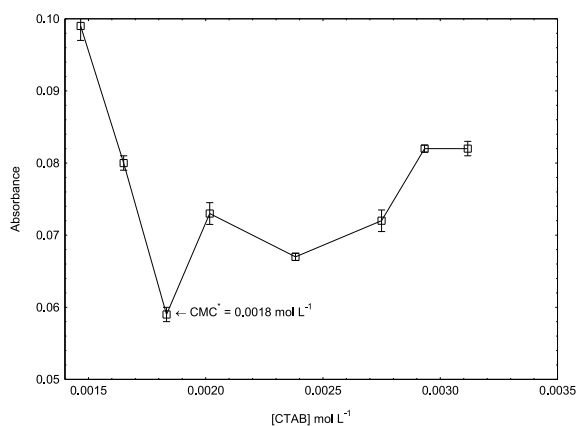**Fig. 7.** The change in absorbance with various CTAB concentrations in 0.1 v.f.of EtOH–H$_2$O at 298.15 ± 0.2 K.

Fig. 8. The change in absorbance with various CTAB concentrations in 0.2 v.f.of EtOH–H$_2$O at 298.15 ± 0.2 K.
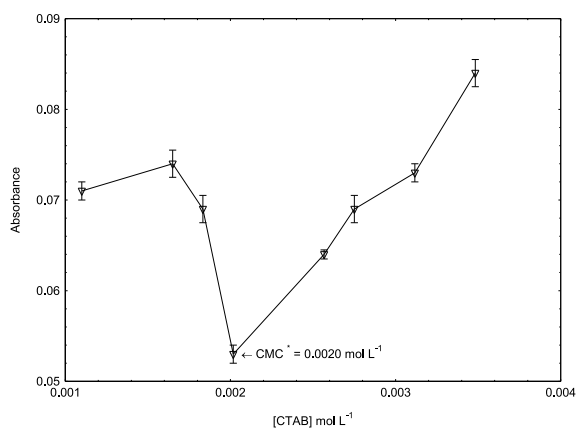

Fig. 9. The change in absorbance with various CTAB concentrations in 0.3 v.f.of EtOH–H$_2$O at 298.15 ± 0.2 K.

[18,19]. Fig. 11 displays the curvilinear swings of ΔG_m^o with the v.f. of ethanol under investigation (i.e. the variation does not follow the linear path but rather a curve). The second-order polynomial equation best fits this curve with r^2 = 0.999. The value of ΔG_m^o is -ve in all the solvent systems under investigation and increases as the concentration of ethanol in the medium increases.

Table 2

Spectral parameters: CMC*, Gibbs energy of micellization, Absorbance, absorption maxima (λ_{max}), Binding constant (K_b), Gibbs energy of binding (ΔG_b^o) for the interaction of methyl red with CTAB micelles in NaPSS in water and in EtOH–H$_2$O binary solvent systems at 298.15 ± 0.2K.

V.f. of Ethanol	CMC* (mol L^{-1})	ΔG_m^o (kJ mol^{-1})	Absorbance at CMC*	λ (nm)	K$_b$ (L mol^{-1})	ΔG_b^o (kJ mol^{-1})
0	0.0011	−16.89	0.016	412–430	461.65	−15.20
0.1	0.0015	−16.17	0.025	410–415	792.37	−16.54
0.2	0.0018	−15.62	0.059	525	980.30	−17.07
0.3	0.0020	−15.38	0.053	520–525	1231.11	−17.63
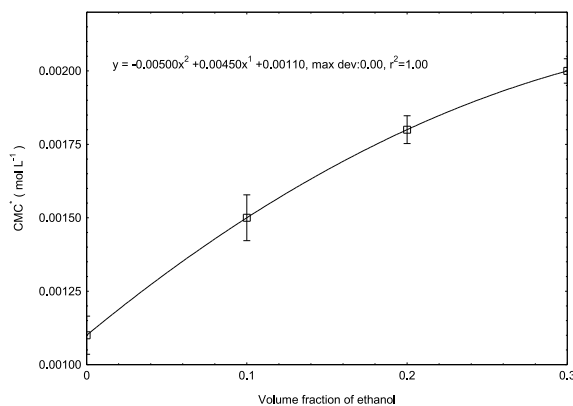
Fig. 10. Variation of CMC* with v.f. of EtOH.
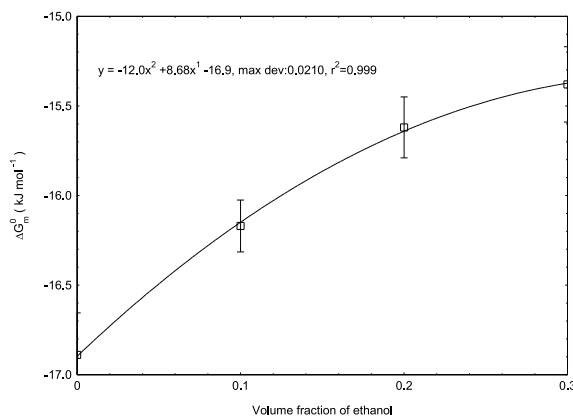
Fig. 11. Variation of Gibbs energy of micellization (ΔG_m^o) versus v.f. of ethanol.

3.3. Calculation of binding constant from spectroscopic data

Determining the binding constant is a crucial step in analyzing and interpreting molecular interactions since it offers a basic indicator of a solute's affinity for a ligand [84]. Stronger interactions between the dye molecules and micelles are predicted by larger values of the binding constant (K$_b$) [16].

The following modified form of the Benesi-Hildebrand Equation [28,39] can be used to quantitatively calculate the binding constant for interaction between CTAB micelles and MR molecules, which is valid for the high concentration of surfactant:

$$\frac{D_T}{\Delta A} = \frac{1}{(\varepsilon_m - \varepsilon_0)} + \frac{1}{K_b (\varepsilon_m - \varepsilon_0) \, C_m} \tag{2}$$

ΔA = A-A$_0$ = Difference in the values of absorbance of methyl red dye in the presence and absence of surfactant in NaPSS, D_T = total concentration of the dye, ε_m = molar extinction coefficient micelle bound dye, ε_0 = molar extinction coefficient of dye, K_b = binding constant, C_m = concentration of CTAB in the micellized conditions where, C_m = C$_s$ - CMC*, and C$_s$ = corresponding concentration of surfactant CTAB under the concentration range investigated

The linear nature of the graphs is obtained from the plot of $\frac{D_T}{\Delta A}$ against $\frac{1}{C_m}$ (Figs. 12, 13, 14, and 15) in every case under investigation. The values of K_b are determined from the slope and are found to be K_b = 461.15, 792.37, 980.3, and 1231.11 L mol^{-1} respectively for water, 0.1, 0.2, and 0.3 v.f. EtOH–H$_2$O (Table 2). The Lambert-Beer law is supported at high concentrations of CTAB by linear correlations (r^2 = 0.9633, 0.9935, 0.9165, and 0.9115) in every case. The increasing values of the binding constant indicate more stronger interaction between MR and CTAB under the influence of NaPSS with increasing alcohol content. Similar trends are also reported in the literature [4,43,50,85].

The following relation is used to calculate the standard Gibbs energy of binding (ΔG_b^o) from K_b value [86].:

$$\Delta G_b^o = -\ RT\ ln\ K_b \tag{3}$$

Where R and T are the molar gas constant and temperature in Kelvin. The decrease in the value of ΔG_b^o (Table 2) further justifies the spontaneous nature of the interaction between MR and CTAB micelles in the post-micellar region.

3.4. Spectroscopic perspectives of the binding properties of MR with CTAB micelles with NaPSS in water and various EtOH–H$_2$O volume fractions

The value of K_b increases in the order: $(K_b)_{\text{water}} < (K_b)_{0.1} < (K_b)_{0.2} < (K_b)_{0.3}$, and ΔG_b^o decreases in the following order: $(\Delta G_b^o)_{\text{water}} > (\Delta G_b^o)_{0.1} > (\Delta G_b^o)_{0.2} > (\Delta G_b^o)_{0.3}$ with increasing concentration of ethanol in the medium (Table 2). These spectroscopic data suggest that the increase in ethanol content in the solvent is favorable for the interaction of MR with CTAB in NaPSS in water and in different EtOH–H$_2$O solvent systems. Similar results were also reported in the literature [25]. The hydrophobically interacting forces between the two different species that react in the post micellar region are weakened on increasing the ethanol content in the medium, but at the same time, the electrostatic interactions become stronger, which leads to an overall increase in the binding constant [25,86].

Despite the weakening of hydrophobic interactions, the rise in K_b values with an increase in ethanol content indicate a major contribution to electrostatic interaction shown by a reduction in ΔG_b^o. The more -ve value of ΔG_b^o further supports the spontaneity of the binding process in the binary solvent media. The plot of K_b versus v.f. of ethanol (Fig. 16), gives the best fitting with correlation coefficient, $r^2 = 1$, which is further supported by the decrease in standard Gibbs energy of binding (ΔG_b^o) (Fig. 17) with increasing ethanol content. The plot of ΔG_b^o versus v.f. of ethanol also gives the best fitting with, $r^2 = 1$. Furthermore, this increase in K_b values demonstrate that the micelle surface in ethanol-mixed solvent enhances the solubilization of the dye within the micelle [19]. Furthermore, by altering the solvent content and raising surfactant concentration after CMC*, micelle size and shape can be changed [71,72]. Therefore, switching from water to ethanol/water solvent systems in the concentration range under study is advantageous since it can enhance the dye's solubilization and the carrier ability of the CTAB.

4. Conclusion

In light of the findings, it is concluded that in the solvent systems (water, 0.1, 0.2, and 0.3 v.f. of EtOH–H$_2$O), the CMC* values obtained from spectroscopic data increase in the order: (CMC* = 0.0011)$_{\text{water}}$ < (CMC* = 0.0015)$_{0.1}$ < (CMC* = 0.0018)$_{0.2}$ < (CMC* = 0.0020)$_{0.3}$. This is because of the reduced polarity or dielectric constant and increased degree of water structure disruption around the hydrophobic chains of CTAB, the micelle formation occurs at somewhat higher concentrations. The less -ve value of Gibbs energy of micellization (ΔG_m^o) : ($\Delta G_m^o = -16.89$ kJ mol^{-1})$_{\text{water}}$ < ($\Delta G_m^o = -16.17$ kJ mol^{-1})$_{0.1.}$ < ($\Delta G_m^o = -15.62$ kJ mol^{-1})$_{0.2}$ < ($\Delta G_m^o = -15.38$ kJ mol^{-1})$_{0.3.}$ further supports the inhibitory effect of increasing ethanol content towards micellization. As the ethanol content in the solvent increases, the hydrophobically interacting forces between the two reacting species in the post-micellar region become less. However, the increased electrostatic interactions lead to a rise in the overall binding constant value. This means that, when NaPSS is present, the stronger electrostatic interactions in the post-micellar region contribute significantly to the increased binding of CTAB
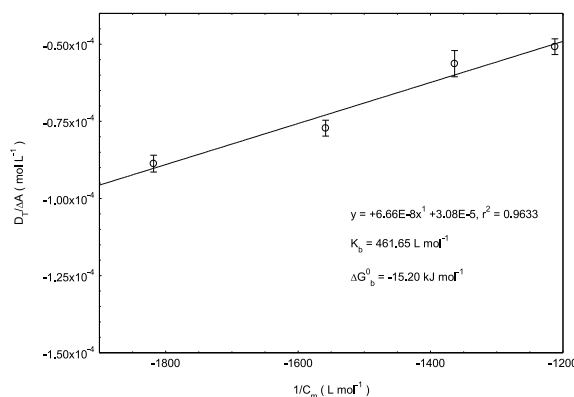

Fig. 12. Plot of D$_T$/ Δ A versus 1/Cm for binding constant calculation in water.
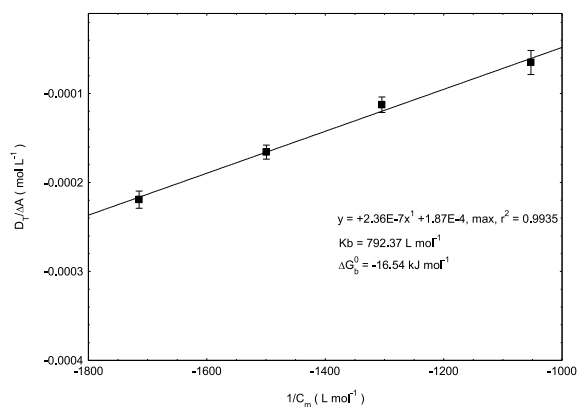
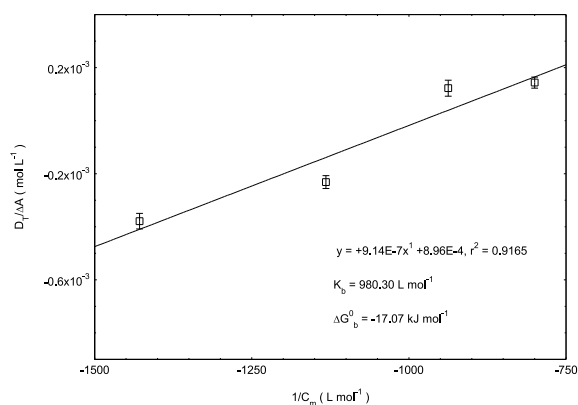**Fig. 13.** Plot of $D_T/\Delta A$ versus $1/Cm$ for binding constant calculation in 0.1 v.f. of EtOH–H_2O.

Fig. 14. Plot of $D_T/\Delta A$ versus $1/Cm$ for binding constant calculation in 0.2 v.f. of EtOH–H_2O.
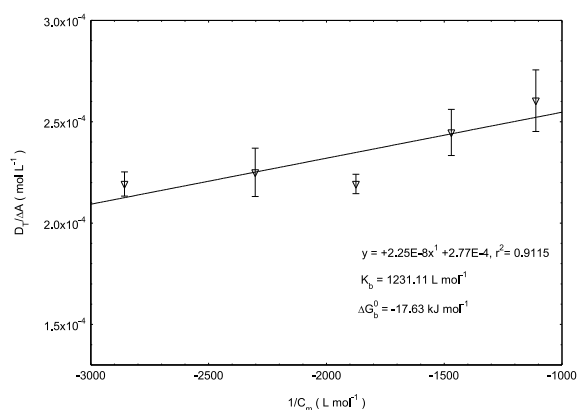

Fig. 15. Plot of $D_T/\Delta A$ versus $1/Cm$ for binding constant calculation in 0.3 v.f. of EtOH–H_2O.

micelles with methyl red, and K_b values follow the order: $(K_b = 461.15)_{water} < (K_b = 792.37)_{0.1} < (K_b = 980.30)_{0.2} < (K_b = 1231.11)_{0.3}$, and ΔG_b^0 decreases in the following order: $(\Delta G_b^o = -15.20 \text{ kJ mol}^{-1})_{water} > (\Delta G_b^o = -16.54 \text{ kJ mol}^{-1})_{0.1} > (\Delta G_b^o = -17.07 \text{ kJ mol}^{-1})_{0.2} > (\Delta G_b^o = -17.63 \text{ kJ mol}^{-1})_{0.3}$. A higher binding constant (K_b) value denotes an enhanced MR-CTAB-NaPSS interaction in the post-micellar region, which is supported by the spontaneity of the process by the decrease in standard Gibbs energy of binding (ΔG_b^o). The tautomeric activity of methyl red (MR), and the solvent composition played the prime role in affecting the interaction mechanism, as evidenced by the blue and red spectral shifts. The findings of this investigation contribute significantly to gaining a
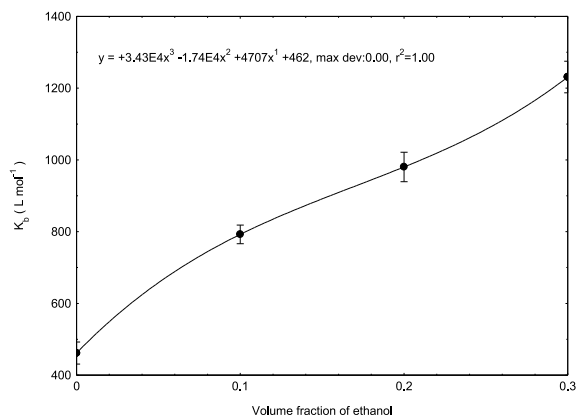
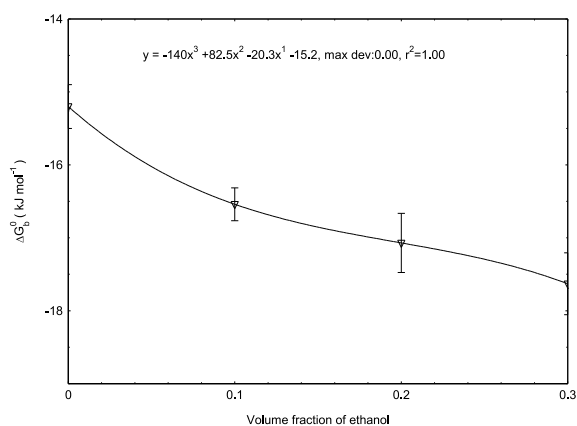**Fig. 16.** Binding constant (K_b) versus v.f. of ethanol.

Fig. 17. Variation of Gibbs energy of binding (ΔG_b^0) versus v.f. of ethanol.

better understanding of the complex molecular interactions and their implications in diverse scientific, industrial, ecological, pharmaceutical, and technological domains. It will also pave the way for future studies on the effects of various co-solvents and other additives in the dye-surfactant-polyelectrolyte (DSP) interaction for the production of new, advanced, and sustainable materials with enhanced yield and economy for relevance to society.

Disclaimer

The findings expressed in this paper are those of the authors alone and do not reflect the official stance of the National Archives, Ministry of Culture, Tourism, and Civil Aviation, Government of Nepal.

Data availability

The data would be available on request from the corresponding author.

CRediT authorship contribution statement

Shiv Narayan Yadav: Writing – original draft, Project administration, Investigation, Data curation. **Summi Rai:** Writing – review & editing, Methodology, Formal analysis, Data curation. **Ajaya Bhattarai:** Writing – review & editing, Software, Resources, Funding acquisition, Conceptualization. **Biswajit Sinha:** Writing – review & editing, Visualization, Validation, Supervision.

Declaration of competing interest

The authors declare that they have no known competing financial interests or personal relationships that could have appeared to

influence the work reported in this paper.

Acknowledgement

References

[1] A. Bhattarai, H. Wilczura-Wachnik, Interaction between morin and AOT reversed micelles - studies with UV-vis at 25°C, Int. J. Pharm. 461 (2014) 14–21, https://doi.org/10.1016/j.ijpharm.2013.11.003.

[2] S. Mahbub, I. Shahriar, M. Iqfath, M.A. Hoque, M.A. Halim, M.A. Khan, M.A. Rub, A.M. Asiri, Influence of alcohols/electrolytes on the interaction of reactive red dye with surfactant and removal of dye from solutions, J. Environ. Chem. Eng. 7 (2019) 103364, https://doi.org/10.1016/j.jece.2019.103364.

[3] M.M. Hosen, S.S. Rakhi, M. Alfakeer, M.M. Rahman, S. Mahbub, M.A. Hoque, D. Kumar, The influence of organic and inorganic additives on the polymer mediated phase separation of triton X-100, J. Mol. Liq. 335 (2021) 116182, https://doi.org/10.1016/j.molliq.2021.116182.

[4] K.M. Sachin, S.A. Karpe, M. Singh, A. Bhattarai, Self-assembly of sodium dodecylsulfate and dodecyltrimethylammonium bromide mixed surfactants with dyes in aqueous mixtures, R. Soc. Open Sci. 6 (2019), https://doi.org/10.1098/rsos.181979.

[5] F. Gul, A.M. Khan, S.S. Shah, M.F. Nazar, Spectroscopic study of alizarin red s binding with cetyltrimethylammonium bromide at low concentrations, Color. Technol. 126 (2010) 109–113, https://doi.org/10.1111/j.1478-4408.2010.00236.x.

[6] F. Schulze-Zachau, B. Braunschweig, CnTAB/polystyrene sulfonate mixtures at air-water interfaces: effects of alkyl chain length on surface activity and charging state, Phys. Chem. Chem. Phys. 21 (2019) 7847–7856, https://doi.org/10.1039/c9cp01107b.

[7] K. Majewska-Nowak, The effect of a polyelectrolyte on the efficiency of dye-surfactant solution treatment by ultrafiltration, Desalination 221 (2008) 395–404, https://doi.org/10.1016/j.desal.2007.02.057.

[8] V. Katheresan, J. Kansedo, S.Y. Lau, Efficiency of various recent wastewater dye removal methods: a review, J. Environ. Chem. Eng. 6 (2018) 4676–4697, https://doi.org/10.1016/j.jece.2018.06.060.

[9] A.C. Benchea, D. Babusca, Č. Podlipnik, D.G. Dimitriu, Solvatochromic and quantum-mechanical characterization of methyl red, Anal. Lett. 50 (2017) 2711–2724, https://doi.org/10.1080/00032719.2017.1296852.

[10] J.H. Zhang, Q. Liu, Y.M. Chen, Z.Q. Liu, C.W. Xu, Determination of acid dissociation constant of methyl red by multi-peaks Gaussian fitting method based on UV-visible absorption spectrum, Wuli Huaxue Xuebao/Acta Phys. - Chim. Sin. 28 (2012) 1030–1036, https://doi.org/10.3866/PKU.WHXB201203025.

[11] M.R. Plutino, E. Guido, C. Colleoni, G. Rosace, Effect of GPTMS functionalization on the improvement of the PH-sensitive methyl red photostability, Sensor. Actuator. B Chem. 238 (2017) 281–291, https://doi.org/10.1016/j.snb.2016.07.050.

[12] S. Sharifi, M.F. Nazar, F. Rakhshanizadeh, S.A. Sangsefedi, A. Azarpour, Impact of amino acids, organic solvents and surfactants on azo-hydrazone tautomerism in methyl red: spectral-luminescent and nonlinear optical properties, Opt. Quant. Electron. 52 (2020), https://doi.org/10.1007/s11082-020-2211-3.

[13] G. Prasad Tajpuriya, P. Shah, N. Shahi, A. Bhattarai, UV–Vis studies of methyl red in the presence of sodium dioctylsulfosuccinate/acetone and sodium dioctylsulfosuccinate/acetone/water, Spectrochim. Acta Part A Mol. Biomol. Spectrosc. 255 (2021) 119646, https://doi.org/10.1016/j.saa.2021.119646.

[14] C.S. Hodges, S. Biggs, L. Walker, Complex adsorption behavior of rodlike polyelectrolyte - surfactant aggregates, Langmuir 25 (2009) 4484–4489, https://doi.org/10.1021/la8033534.

[15] V. Abbot, P. Sharma, Investigating thermodynamic, acoustic and spectroscopic parameters of rutin trihydrate with cationic surfactant CTAB in hydro-ethanolic solvent systems, J. Mol. Liq. 328 (2021) 115489, https://doi.org/10.1016/j.molliq.2021.115489.

[16] S. Noor, M.B. Taj, A. Ashar, Solubilization of cationic dye in single and mixed micellar media, J. Mol. Liq. 330 (2021) 115613, https://doi.org/10.1016/j.molliq.2021.115613.

[17] K. Kogej, Polyelectrolytes and surfactants in aqueous solutions. From dilute to concentrated systems, in: Advances in Planar Lipid Bilayers and Liposomes;, vol 16, Elsevier Inc., 2012, pp. 199–237. ISBN 9780123965349.

[18] A. Bhattarai, Micellization behavior of cetyltrimethylammonium bromide in the absence and presence of sodium polystyrene sulfonate in water and methanol-water mixture: a conductivity approach, J. Mol. Liq. 292 (2019) 111352, https://doi.org/10.1016/j.molliq.2019.111352.

[19] A. Bhattarai, Studies of aggregation properties of surfactant with and without polyelectrolyte in water and binary mixture of methanol-water from the surface tension measurements, J. Mol. Liq. 312 (2020) 113438, https://doi.org/10.1016/j.molliq.2020.113438.

[20] K.M. Sachin, S.A. Karpe, M. Singh, A. Bhattarai, An interaction of anionic- and cationic-rich mixed surfactants in aqueous medium through physicochemical properties at three different temperatures, J. Chem. 2018 (2018), https://doi.org/10.1155/2018/4594062.

[21] K. Kumar, S. Chauhan, Volumetric, compressibility and viscometric studies on sodium cholate/sodium deoxycholate-amino acid interactions in aqueous medium, Thermochim. Acta 606 (2015) 12–24, https://doi.org/10.1016/j.tca.2015.02.014.

[22] S. Narayan Yadav, S. Rai, P. Shah, N. Roy, A. Bhattarai, Spectrophotometric and conductometric studies on the interaction of surfactant with polyelectrolyte in the presence of dye in aqueous medium, J. Mol. Liq. 355 (2022) 118949, https://doi.org/10.1016/j.molliq.2022.118949.

[23] Z.H. Asadov, R.A. Rahimov, T.A. Poladova, S.M. Nasibova, A.D. Guliyev, A.Z. Asadova, Triethylenetetramine-based novel cationic surfactants and their complexes with anionic polyelectrolytes, J. Mol. Liq. 166 (2012) 44–48, https://doi.org/10.1016/j.molliq.2011.11.011.

[24] S. Tul-Muntaha, M.N. Khan, Conductometric investigation of the interaction of natural and synthetic surfactant with cationic dye in water-alcohol mixed solvent, J. Chem. Eng. Data 60 (2015) 3009–3017, https://doi.org/10.1021/acs.jced.5b00434.

[25] T.S. Banipal, H. Kaur, P.K. Banipal, Studies on the binding ability of diclofenac sodium to cationic surfactants micelles in aqueous ethanol solutions: calorimetric, spectroscopic, and light scattering approach, J. Therm. Anal. Calorim. 128 (2017) 501–511, https://doi.org/10.1007/s10973-016-5889-5.

[26] H. Ouni, A. Hafiane, M. Dhahbi, The effect of surfactant on dye removal by polyelectrolyte enhanced ultrafiltration, Desalination Water Treat. 56 (2015) 1526–1535, https://doi.org/10.1080/19443994.2014.952670.

[27] A. Ali, S. Uzair, U. Farooq, M. Ali, Effect of tartrazine dye on micellisation of cationic surfactants: conductometric, spectrophotometric, and tensiometric studies, Color. Technol. 132 (2016) 376–386, https://doi.org/10.1111/cote.12229.

[28] M.S. Ramadan, N.M. El-Mallah, G.M. Nabil, S.M. Abd-Elmenem, Hydrophobic effect for anionic dye - cationic surfactant interaction in aqueous and mixed solvent, J. Dispersion Sci. Technol. 40 (2019) 1110–1120, https://doi.org/10.1080/01932691.2018.1496837.

[29] Z. Khan, M.A. Malik, S.A. Al-Thabaiti, A. Alshehri, F. Nabi, Micellization and thermodynamic properties of cationic surfactant cetyltrimethylammonium bromide in non-aqueous mixture of lauric acid, Int. J. Electrochem. Sci. 12 (2017) 4528–4542, https://doi.org/10.20964/2017.05.53.

[30] M. Bielawska, A. Chodzińska, B. Jańczuk, A. Zdziennicka, Determination of CTAB CMC in mixed water+short-chain alcohol solvent by surface tension, conductivity, density and viscosity measurements, Colloids Surfaces A Physicochem. Eng. Asp. 424 (2013) 81–88, https://doi.org/10.1016/j.colsurfa.2013.02.017.

[31] W. Li, Y.C. Han, J.L. Zhang, B.G. Wang, Effect of ethanol on the aggregation properties of cetyltrimethylammonium bromide surfactant, Colloid J. 67 (2005) 159–163, https://doi.org/10.1007/s10595-005-0075-7.

[32] L. Brinchi, P. Di Profio, R. Germani, G. Savelli, N. Spreti, Effect of ethanol on micellization and on decarboxylation of 6-nitrobenzisoxazole-3-carboxylate in aqueous cationic micelles, J. Colloid Interface Sci. 247 (2002) 429–436, https://doi.org/10.1006/jcis.2001.8053.

[33] S. Das, S. Mondal, S. Ghosh, Physicochemical studies on the micellization of cationic, anionic, and nonionic surfactants in water-polar organic solvent mixtures, J. Chem. Eng. Data 58 (2013) 2586–2595, https://doi.org/10.1021/je4004788.

[34] S. Ben Mahmoud, A.H. Hamzaoui, W. Essafi, Spectrophotometric study of the interaction of methylene blue with poly(styrene-Co-sodium styrene sulfonate, Mediterr. J. Chem. 5 (2016) 493–506, https://doi.org/10.13171/mjc54/01606162106/essafi.

[35] M.M. Mabrouk, N.A. Hamed, F.R. Mansour, Spectroscopic methods for determination of critical micelle concentrations of surfactants; a comprehensive review, Appl. Spectrosc. Rev. 58 (2023) 206–234, https://doi.org/10.1080/05704928.2021.1955702.

[36] M.A. Rather, G.M. Rather, S.A. Pandit, S.A. Bhat, M.A. Bhat, Determination of cmc of imidazolium based surface active ionic liquids through probe-less UV-vis spectrophotometry, Talanta 131 (2015) 55–58, https://doi.org/10.1016/j.talanta.2014.07.046.

[37] G.A. Ahmadova, R.A. Rahimov, A.Z. Abilova, K.A. Huseynova, E. Imanov, F.I. Zubkov, Effect of head-group of cationic surfactants and structure of ionic groups of anionic polyelectrolyte in oppositely charged polymer-surfactant complexes, Colloids Surfaces A Physicochem. Eng. Asp. 613 (2021) 126075, https://doi.org/10.1016/j.colsurfa.2020.126075.

[38] T. Chakraborty, I. Chakraborty, S. Ghosh, Sodium carboxymethylcellulose - CTAB interaction: a detailed thermodynamic study of polymer - surfactant interaction with opposite charges, Langmuir 22 (2006) 9905–9913, https://doi.org/10.1021/la0621214.

[39] K. Edbey, A. El-Hashani, A. Benhmid, K. Ghwel, M. Benamer, Spectral studies of eriochrome black T in cationic surfactants, Chem. Sci. Int. J. 24 (2018) 1–12, https://doi.org/10.9734/csji/2018/44312.

[40] B. Khadka, A. Bhattarai, Uv-vis studies on interaction between sodium dioctylsulfosuccinate (aot) and methyl red, Rev. Roum. Chem. 65 (2020) 989–996, https://doi.org/10.33224/rrch.2020.65.11.04.

[41] R. Nandini, B.A. Vishalakshi, Comparitive study of polyelectrolyte-dye interactions, Spectrochim. Acta Part A Mol. Biomol. Spectrosc. 74 (2009) 1025–1030, https://doi.org/10.1016/j.saa.2009.08.043.

[42] A.M. Khan, S. Bashir, A. Shah, M.F. Nazar, H.M.A. Rahman, S.S. Shah, A.Y. Khan, A.R. Khan, F. Shah, Spectroscopically probing the effects of holmium(III) based complex counterion on the dye-cationic surfactant interactions, Colloids Surfaces A Physicochem. Eng. Asp. 539 (2018) 407–415, https://doi.org/10.1016/j.colsurfa.2017.12.023.

[43] A. Ben Fradj, R. Lafi, S. Ben Hamouda, L. Gzara, A.H. Hamzaoui, A. Hafiane, Investigation on the interaction of safranin T with anionic polyelectrolytes by spectrophotometric method, Spectrochim. Acta Part A Mol. Biomol. Spectrosc. 131 (2014) 169–176, https://doi.org/10.1016/j.saa.2014.04.028.

[44] R.K. Srour, L.M. McDonald, Determination of the acidity constants of methyl red and phenol red indicators in binary methanol - and ethanol-water mixtures, J. Chem. Eng. Data 53 (2008) 116–127, https://doi.org/10.1021/je700413x.

[45] A.R. Tehrani-Bagha, K. Holmberg, Solubilization of hydrophobic dyes in surfactant solutions, Materials 6 (2013) 580–608, https://doi.org/10.3390/ma6020580.

[46] S. Younis, M. Usman, ul Haq Atta, N. Akram, M. Saeed, S. Raza, M. Siddiq, F. Bukhtawar, Solubilization of reactive dyes by mixed micellar system: synergistic effect of nonionic surfactant on solubilizing power of cationic surfactant, Chem. Phys. Lett. 738 (2020) 136890, https://doi.org/10.1016/j.cplett.2019.136890.

[47] J.K. Salem, I.M. El-Nahhal, S.F. Salama, Determination of the critical micelle concentration by absorbance and fluorescence techniques using fluorescein probe, Chem. Phys. Lett. 730 (2019) 445–450, https://doi.org/10.1016/j.cplett.2019.06.018.

[48] V. Kumar, D. Patel, H.A. Pal, Comprehensive Insight on H-type Aggregation in Congo Red-Surfactant Systems Revealed through Spectroscopic and Electrochemical Study Unified, 2019, pp. 15584–15594, https://doi.org/10.1039/c9cp00482c.

[49] P.K. Paul, S.A. Hussain, D. Bhattacharjee, M. Pal, Adsorption of cationic laser dye onto polymer/surfactant complex film, Chin. J. Chem. Phys. 24 (2011) 348–352, https://doi.org/10.1088/1674-0068/24/03/348-352.

[50] A. Ben Fradj, R. Lafi, L. Gzara, A.H. Hamzaoui, A. Hafiane, Spectrophotometric study of the interaction of toluidine blue with poly (ammonium acrylate), J. Mol. Liq. 194 (2014) 110–114, https://doi.org/10.1016/j.molliq.2014.01.008.

[51] M. Irfan, M. Usman, A. Mansha, N. Rasool, M. Ibrahim, U.A. Rana, M. Siddiq, M. Zia-Ul-Haq, H.Z.E. Jaafar, S.U.D. Khan, Thermodynamic and spectroscopic investigation of interactions between reactive red 223 and reactive orange 122 anionic dyes and cetyltrimethyl ammonium bromide (CTAB) cationic surfactant in aqueous solution, Sci. World J. (2014), https://doi.org/10.1155/2014/540975, 2014.

[52] A. Mitra, R.K. Nath, S. Biswas, A.K. Chakraborty, A.K. Panda, A comparative study on the physico-chemical properties of bacterial capsular polysaccharides from different serotypes of Klebsiella, J. Photochem. Photobiol. Chem. 178 (2006) 98–105, https://doi.org/10.1016/J.JPHOTOCHEM.2005.07.006.

[53] M. Taj Muhammad, M.N. Khan, Study of electrolytic effect on the interaction between anionic surfactant and methylene blue using spectrophotometric and conductivity methods, J. Mol. Liq. 234 (2017) 309–314, https://doi.org/10.1016/j.molliq.2017.03.102.

[54] M. Khamis, B. Bulos, F. Jumean, A. Manassra, M. Dakiky, Azo dyes interactions with surfactants. Determination of the critical micelle concentration from acid-base equilibrium, Dyes Pigments 66 (2005) 179–183, https://doi.org/10.1016/j.dyepig.2004.09.012.

[55] N. Zaghbani, M. Dhahbi, A. Hafiane, Spectral study of eriochrome blue black R in different cationic surfactant solutions, Spectrochim. Acta Part A Mol. Biomol. Spectrosc. 79 (2011) 1528–1531, https://doi.org/10.1016/j.saa.2011.05.011.

[56] S.S. Shah, G.M. Laghari, K. Naeem, Spectroscopic study of hemicyanine dyes in anionic micellar solutions, Thin Solid Films 346 (1999) 145–149, https://doi.org/10.1016/S0040-6090(98)01773-8.

[57] S. Chandravanshi, S.K. Upadhyay, Natural dye-surfactant interactions: thermodynamic and surface parameters, Color. Technol. 128 (2012) 300–305, https://doi.org/10.1111/j.1478-4408.2012.00380.x.

[58] S. Sharifi, Muhammad, F. Nazar, Forough Rakhshanizadeh, Seyed, A. Sangsefedi, A. Azarpour, Impact of amino acids, Organic Solvents and Surfactants on Azo-Hydrazone Tautomerism in Methyl Red: Spectral-Luminescent and Nonlinear Optical Properties 52 (2020) 98, https://doi.org/10.1007/s11082-020-2211-3.

[59] P. Shah, S. Kumari Jha, A. Bhattarai, Spectrophotometric study of the sodium dodecyl sulfate in the presence of methylene blue in the methanol–water mixed solvent system, J. Mol. Liq. 340 (2021) 117200, https://doi.org/10.1016/j.molliq.2021.117200.

[60] J. Oakes, P. Gratton, Solubilisation of dyes by surfactant micelles. Part 1: molecular interactions of azo dyes with nonionic and anionic surfactants, Color. Technol. 119 (2003) 91–99, https://doi.org/10.1111/j.1478-4408.2003.tb00156.x.

[61] Z. Zhao, F.C. Spano, Vibronic fine structure in the absorption spectrum of oligothiophene thin films, J. Chem. Phys. 122 (2005), https://doi.org/10.1063/1.1861456.

[62] D. González-Arjona, G. López-Pérez, M.M. Domínguez, A.G. González, Solvatochromism: a comprehensive Project for the final year undergraduate chemistry laboratory, J. Lab. Chem. Educ. 2016 (2016) 45–52, https://doi.org/10.5923/j.jlce.20160403.01.

[63] S. Hanif, M. Usman, A. Hussain, N. Rasool, M. Zubair, U.A. Rana, Solubilization of benzothiazole (BNZ) by micellar media of sodium dodecyl sulphate and cetyl trimethylammonium bromide, J. Mol. Liq. 211 (2015) 7–14, https://doi.org/10.1016/j.molliq.2015.06.018.

[64] G.B. Behera, P.K. Behera, B.K. Mishra, Cyanine dyes : self aggregation and behaviour in surfactants: a review, J. Surf. Sci. Technol. 23 (2007) 1–31.

[65] K.K. Karukstis, L.A. Perelman, W.K. Wong, Spectroscopic characterization of azo dye aggregation on dendrimer surfaces, Langmuir 18 (2002) 10363–10371, https://doi.org/10.1021/la020558f.

[66] S.S. Hemdan, A.M. Al Jebaly, F.K. Ali, Importance of isosbestic point in spectroscopy:, A review, 2019) 1 الإنسانية والدراسات العلوم مجلة), https://doi.org/10.37376/1571-000-062-004.

[67] E.H. Mohamed, H.M. Lotfy, M.A. Hegazy, S. Mowaka, Different applications of isosbestic points, normalized spectra and dual wavelength as powerful tools for resolution of multicomponent mixtures with severely overlapping spectra, Chem. Cent. J. 11 (2017) 1–15, https://doi.org/10.1186/s13065-017-0270-8.

[68] T.S. Banipal, H. Kaur, P.K. Banipal, A.K. Sood, Effect of head groups, temperature, and polymer concentration on surfactant - polymer interactions, J. Surfactants Deterg. 17 (2014) 1181–1191, https://doi.org/10.1007/s11743-014-1633-y.

[69] M.F. Nazar, S.S. Shah, M.A. Khosa, Interaction of azo dye with cationic surfactant under different PH conditions, J. Surfactants Deterg. 13 (2010) 529–537, https://doi.org/10.1007/s11743-009-1177-8.

[70] B. Gohain, B. Boruah, P.M. Saikia, R.K. Dutta, Premicellar and micelle formation behavior of aqueous anionic surfactants in the presence of triphenylmethane dyes: protonation of dye in ion pair micelles, J. Phys. Org. Chem. 23 (2010) 211–219, https://doi.org/10.1002/poc.1603.

[71] T. Sidim, G. Acar, Alcohols effect on critic micelle concentration of polysorbate 20 and cetyl trimethyl ammonium bromine mixed solutions, J. Surfactants Deterg. 16 (2013) 601–607, https://doi.org/10.1007/s11743-012-1429-x.

[72] J.B. Huang, M. Mao, B.Y. Zhu, The surface physico-chemical properties of surfactants in ethanol-water mixtures, Colloids Surfaces A Physicochem. Eng. Asp. 155 (1999) 339–348, https://doi.org/10.1016/S0927-7757(99)00003-5.

[73] S. Göktürk, U. Var, Effect of pharmaceutically important cosolvents on the interaction of promethazine and trifluopromazine hydrochloride with sodium dodecyl sulfate micelles, J. Dispersion Sci. Technol. 33 (2012) 527–535, https://doi.org/10.1080/01932691.2011.574934.

[74] S. Rai, A. Kafle, H.P. Devkota, A. Bhattarai, Characterization of saponins from the leaves and stem bark of jatropha curcas L. For surface-active properties, Heliyon 9 (2023) e15807, https://doi.org/10.1016/j.heliyon.2023.e15807.

[75] M.E. Mahmood, D. a F. Al-koofee, Effect of temperature changes on critical micelle concentration for tween series surfactant, Glob. J. Sci. Front. Res. Chem. 13 (2013) 1–7.

[76] A.A. Ansari, M. Kamil, Kabir-ud-Din polymer-surfactant interactions and the effect of tail size variation on micellization process of cationic ATAB surfactants in aqueous medium, J. Dispersion Sci. Technol. 34 (2013) 722–730, https://doi.org/10.1080/01932691.2012.685850.

[77] R. Zieliński, S. Ikeda, H. Nomura, S. Kato, Effect of temperature on micelle formation in aqueous solutions of alkyltrimethylammonium bromides, J. Colloid Interface Sci. 129 (1989) 175–184, https://doi.org/10.1016/0021-9797(89)90428-1.

[78] K. Szutkowski, Z. Kołodziejska, Z. Pietralik, I. Zhukov, A. Skrzypczak, K. Materna, M. Kozak, Clear distinction between CAC and CMC revealed by high-resolution NMR diffusometry for a series of bis-imidazolium gemini surfactants in aqueous solutions, RSC Adv. 8 (2018) 38470–38482, https://doi.org/10.1039/c8ra07081d.

[79] T.D.A. Senra, A. Khoukh, J. Desbrières, Interactions between quaternized chitosan and surfactant studied by diffusion NMR and conductivity, Carbohydr. Polym. 156 (2017) 182–192, https://doi.org/10.1016/j.carbpol.2016.09.025.

[80] D. Li, X. Qian, C. Lian, R. Huang, Z. Hao, M. Cheng, S. Li, C. Li, S. Iqbal, L. Qin, et al., Carbon quantum dots as fluorescent probes in the measurement of the critical micelle concentration of surfactants, Colloids Surfaces A Physicochem. Eng. Asp. 679 (2023) 132584, https://doi.org/10.1016/J.COLSURFA.2023.132584.

[81] S. Narayan, S. Rai, A. Bhattarai, B. Sinha, Impact of sodium polystyrene sulfonate on micellization behaviour of cetyltrimethylammonium bromide in the presence of methyl red in ethanol – water mixture : a conductometric investigation, J. Mol. Liq. 399 (2024) 124387, https://doi.org/10.1016/j.molliq.2024.124387.

[82] Warren solvophobic interactions and micelle formation in structure forming nonaqueous solvents, Nature 231 (1971) 313–315.

[83] H. Akbaş, Ç. Kartal, Conductometric studies of hexadecyltrimethylammonium bromide in aqueous solutions of ethanol and ethylene glycol, Colloid J. 68 (2006) 125–130, https://doi.org/10.1134/S1061933X06020013.

[84] Z. Chen, S.G. Weber, Determination of binding constants by affinity capillary electrophoresis, electrospray ionization mass spectrometry and phase-distribution methods, TrAC, Trends Anal. Chem. 27 (2008) 738–748, https://doi.org/10.1016/j.trac.2008.06.008.

[85] K.M. Sachin, S.A. Karpe, M. Singh, A. Bhattarai, Study on surface properties of sodiumdodecyl sulfate and dodecyltrimethylammonium bromide mixed surfactants and their interaction with dyes, Heliyon 5 (2019) e01510, https://doi.org/10.1016/j.heliyon.2019.e01510.

[86] N. Hashemi, G. Sun, Intermolecular interactions between surfactants and cationic dyes and effect on antimicrobial properties, Ind. Eng. Chem. Res. 49 (2010) 8347–8352, https://doi.org/10.1021/ie101001d.